Adult excitation-neurogenesis coupling: mechanisms and implications

Karl Deisseroth†*#, Sheela Singla*#, Hiroki Toda¶, Michelle Monje¶,
Theo D. Palmer¶, and Robert C. Malenka†#

#Nancy Pritzker Laboratory, Department of Psychiatry and Behavioral Sciences and
¶Department of Neurosurgery, Stanford University School of Medicine, Stanford, CA 94305.

*These authors contributed equally

†Correspondence to:
R.C. Malenka, K. Deisseroth
Dept. of Psychiatry and Behavioral Sciences
1201 Welch Rd., Room P105
Stanford Medical Center
Palo Alto, CA. 94304
650-724-2730
650-724-2753 (fax)
malenka@stanford.edu
deissero@stanford.edu

A wide variety of *in vivo* manipulations influence neurogenesis in the hippocampus. It is not known, however, if adult stem cells or adult stem cell-derived progenitor cells can intrinsically sense neural activity and thereby implement a direct coupling between excitation and neurogenesis. Moreover, theoretical frameworks are lacking to predict the consequences of activity-dependent insertion of new neurons into pre-existing networks. Here we demonstrate that excitatory stimuli act directly on adult hippocampal stem/progenitor cells to favor neurogenesis. Excitation sensed via $Ca_v1.2/1.3$ (L-type) Ca^{2+} channels and NMDA receptors initiates a proneural gene expression program in proliferating progenitor cells and instructively drives increased neurogenesis. Incorporation of the progenitor cells' activity-sensing properties as an "excitation-neurogenesis coupling rule" within a Hebbian neural network predicts significant advantages of activity-coupled neurogenesis for both the temporary storage and the clearance of memories.

It is well established that in certain areas of the adult brain, proliferating cells continually give rise to new neurons, a process termed neurogenesis. In the hippocampus, neurogenesis is influenced by a variety of conditions(1-4), but it is unknown if activity is meaningfully coupled to neurogenesis to allow adaptive plasticity of hippocampal neural circuits at the cellular level. A provocative possibility is that actively proliferating adult progenitors have the ability to directly detect and respond to particular patterns of excitatory activity passing through the neural network in which they are embedded, perhaps by making computationally appropriate cell phenotype decisions. Instructive influences of activity in the adult would contrast with embryonic development, where neural progenitor cells mediate grossly normal development in the absence of key activity signals (5, 6). An instructive influence of activity on neurogenesis would have particular importance in the adult since production of new neurons may mediate complex physiological brain functions(3, 4, 7-11) including the storage(12) and clearance(13) of memories. Furthermore**,** while deranged neurogenesis may contribute to brain disorders ranging from epilepsy(14) to depression(15), adult neurogenesis might nonetheless be productively harnessed for therapeutic purposes(16, 17).

Conditions known to modulate proliferation and survival(8) of adult progenitor cells are diverse, and include seizure(14, 15, 18), stroke(1, 19), behavioral stimuli(8, 20), adrenalectomy(2), antidepressants(15), and NMDA receptor blockade(8, 21). Many of these interventions in principle could act by modulating activity levels in the hippocampus. For example, acute NMDA receptor blockade causes an increase in proliferation-dependent neurogenesis(8, 21). It is not known, however, if this excitatory receptor blockade actually translates into decreased hippocampal activity. In fact, other global interventions, which might be expected to increase activity (e.g. running, status epilepticus, enriched environments) (14, 15,

18, 20), paradoxically also increase proliferation and resulting neurogenesis. Many potential complicating factors, such as cell death and release of cytokines, make it difficult to determine if changes in activity *per se* actually have any direct effects on the proliferating progenitor cells themselves. An additional critical issue is whether the resulting mature cell phenotype, rather than proliferation alone, is controlled by activity, as not all newborn cells become neurons (10, 22, 23).

Using an array of approaches both *in vitro* and *in vivo* we have addressed several fundamental questions about the role of activity in controlling adult neurogenesis: (1) are proliferating adult progenitor cells themselves computational elements capable of responding to local activity signals? (2) how are these signals transduced to influence the production of new neurons? (3) what are the rules governing excitation-neurogenesis coupling (if any)? and (4) what are the computational advantages for the functioning of mature brain networks of having excitation-neurogenesis coupling?

Excitation promotes neurogenesis from adult stem/progenitor cells

Previous *in vivo* manipulations thought to influence hippocampal activity typically have involved global delivery of phasic or transient stimuli; significant effects on proliferation are seen but, as noted above, the results do not fit into a consistent pattern (8). Although this work on adult neurogenesis is clearly important, there are several unavoidable but major limitations to examining, *in vivo*, the effects of activity on neurogenesis. First, it is difficult to know how hippocampal network activity is actually affected by global *in vivo* manipulations without extensive electrophysiological recordings. Second, it is difficult to precisely control activity levels in a rigorous fashion in awake, behaving animals. Third, it is difficult *in vivo* to determine

which cell type(s) directly sense any changes in activity and thereby influence neurogenesis. Fourth, it is also difficult to elucidate the detailed molecular mechanisms responsible for any effects of activity on neurogenesis. Therefore, to directly determine the neurogenic effects of activity on proliferating adult stem/progenitor cells (which we term excitation-neurogenesis coupling), we turned to a reduced *in vitro* system which provided experimental control over the cellular environment to an extent not possible *in vivo*. This allowed us to provide uniform proliferative conditions and defined excitation and differentiation stimuli as well as conduct full physiological characterization of the functional status of the resulting differentiated cells.

To examine stem/progenitor cell behavior in the presence of mature neurons and glia, we plated a well-characterized(22) green fluorescent protein (GFP)-labeled adult rat hippocampal neural stem/progenitor cell preparation onto a culture of mixed primary hippocampal neurons and glia under mitogenic conditions. The stem/progenitor cells were low passage cultures of cells isolated directly from adult rat hippocampus and have been shown to retain stem cell phenotypes *in vitro* as well as to behave identically to endogenous stem/progenitor cells, (e.g., they participate normally in hippocampal neurogenesis when implanted into the intact hippocampus(24)). One day after plating (termed day 1) the medium was replaced with medium that permitted differentiation(25). As previously reported(23), several measures indicated that neurogenesis was greatly enhanced in primary hippocampal neuron coculture relative to cultures of isolated stem/progenitor cells (Fig. 1A). Specifically, the neuronal dendritic protein MAP2ab was expressed in a much greater proportion of the resulting cells (Fig. 1A-C), tetrodotoxin (TTX)-sensitive voltage-gated Na^+ currents were greatly enhanced (Fig. 1D-F), synaptic currents were recorded (Fig. 2D), and high levels of MAP2ab expression correlated with neuronal morphology (2-5 well-defined primary processes per cell; Fig. 1G).

To mimic the effects of increasing activity to determine its effects on neurogenesis, we next applied mildly depolarizing levels of extracellular potassium to the cocultures at the onset of differentiation on day 1. This caused a striking increase in the fraction of cells that became neurons, as measured by expression of MAP2ab (Fig. 1H, 2A) and the neuronal structural protein Doublecortin (Dcx) (Fig. 2B,C), as well as by the presence of synaptic currents (Fig. 2D). Interestingly, the same stimulus applied in pure stem/progenitor cultures did not increase neurogenesis (Fig. 1H). Therefore, the cellular environment is important not only for promoting adult neurogenesis(23), but also is critical for allowing a further potent excitation-neurogenesis coupling. Direct application of the excitatory neurotransmitter glutamate, also gave rise to an increase in the fraction of cells becoming neurons (Fig. 2A, 2D) indicating that the increased neurogenesis was independent of the method of excitation. To test whether the observed adult excitation-neurogenesis coupling was generalizable to other stem/progenitor cell preparations, we used an independently derived early-passage adult hippocampal stem/progenitor cell population (RH-1)(25). Excitatory stimuli also promoted neurogenesis in this line (data not shown) as evidenced by the increased proportion of cells with MAP2ab expression.

Several lines of evidence indicated that the effect of excitation on the proliferating cells is an instructive influence that promotes the *de novo* production of neurons. First, the effect was not simply a result of a depolarization-induced global increase in the rate or extent of differentiation, as the high-expressing neuronal population continued to express the same level of MAP2ab, independent of the level of stimulation (Fig. 1I, 2A), as did the low-expressing non-neuronal cells (data not shown). Similar results were seen with voltage-gated Na^+ current density (data not shown). Excitation instead induced a large increase in the fraction of the population expressing neuronal MAP2ab levels (Fig. 1I, 2A). Second, the effect of excitation was not simply on

MAP2ab gene expression since expression of the structurally and functionally distinct neuron-specific protein Dcx (Fig. 2B) strongly correlated with MAP2ab (Fig. 2C). In the adult hippocampus, Dcx is expressed in newborn neurons (Fig. 2B), peaking soon after the last cell division and disappearing within a few weeks as newborn neurons become more mature(26). Third, excitation with glutamate or depolarization caused an increase in the fraction of cells that received functional excitatory synaptic connections, determined electrophysiologically with whole-cell patch clamp recording (Fig. 2D). This clearly indicates that depolarization increased the fraction of cells adopting the neuronal lineage. Finally, the increase in the fraction of newborn neurons appeared to be due to instructive changes in the stem/progenitor cell behavior rather than selection for a neuronal subpopulation since there was no detectable effect of excitatory stimuli on the proliferation or survival of cells. Final total cell counts were not increased by depolarization nor were indices of cell death or proliferation influenced by depolarization (Fig. 1I shows representative raw data of final total cell counts: 937 total stem/progenitor derived progeny in the depolarized culture and 1032 in the control; see Fig. 4 for summary of proliferation, survival, and apopotosis measures over many experiments). Taken together, these data demonstrate that independent of proliferation or survival, excitatory stimuli instructively favor the production of fully functional neurons from proliferating adult stem/progenitor cells.

Role of Ca^{2+} in excitation-neurogenesis coupling

Excitation by depolarization could act through Ca_v channels, which play a variety of roles in mediating neuronal responses. While $Ca_v2.1$ (N-type) and $Ca_v2.2$ (P/Q-type) Ca^{2+} channels play critical roles in neuronal synaptic transmission, $Ca_v1.2/1.3$ (L-type) channels have been

implicated in neuronal plasticity and survival(27, 28) and play a unique and privileged role among the various Ca^{2+} channel types in non-synaptic membrane-to-nucleus signaling that modulates activity-dependent gene expression programs (28). It is not known, however, which (if any) of these channel types could be involved in adult excitation-neurogenesis coupling. Employing potent and selective antagonists, the dihydropyridine nifedipine to block the $Ca_v1.2/1.3$ Ca^{2+} channels and the peptide antagonist ω-Ctx-MVIIC to block $Ca_v2.1$ and $Ca_v2.2$ Ca^{2+} channels, we found that ω-Ctx-MVIIC did not inhibit neurogenesis (data not shown), while nifedipine reduced basal neurogenesis (Na, Fig. 2E) and completely blocked the depolarization effect on neurogenesis (K, Fig. 2E). These results indicate that $Ca_v1.2/1.3$ channels are necessary for modulating neuron production in response to excitation.

Certain functions of $Ca_v1.2/1.3$ channels can also be served by NMDA receptors (high-affinity glutamate receptors that are permeable to Ca^{2+}); the two channel types often provide overlapping effects, likely due to a common ability to recuit calmodulin signaling(28). NMDA receptors have been strongly implicated in synaptic plasticity(29, 30), gene expression(27), and memory formation(30), and play a role in dentate gyrus cell proliferation(1, 8, 19, 21). However, the sign and magnitude of effects of NMDA receptor antagonists on progenitor cell proliferation *in vivo* have differed widely, depending on the experimental paradigm(1, 8, 19, 21). To test the potential contribution of NMDA receptors to excitation-neurogenesis coupling under a range of controlled conditions *in vitro*, we applied the specific NMDA receptor antagonist D-AP5 which inhibited basal neurogenesis (Na; Fig. 2F) as well as the increase in neurogenesis elicited by depolarization or glutamate treatment when applied concurrently (K, Glu; Fig. 2F). These results indicate that NMDA receptors also can play a role in adult excitation-neurogenesis

coupling, perhaps by recruiting the same pathway as the $Ca_v1.2/1.3$ channels, as in other systems(28).

Direct excitation of adult hippocampal stem/progenitor cells induces full neurogenesis. Coculture with neurons and glia was necessary for excitation-neurogenesis coupling since excitation had no neurogenic effect on stem/progenitor cells grown in isolation (Fig. 1H). Although this coculture system permitted full characterization of the resulting stem/progenitor-derived neurons, it did not allow determination of whether proliferating cells themselves respond directly to excitation with their own ion channels, or instead respond indirectly, via the living hippocampal neurons or glia. To answer this question, we employed another intervention not possible *in vivo.* Specifically, instead of the living hippocampal coculture environment, we used an ethanol-fixed(23) and extensively washed hippocampal culture as substrate, a setting in which the only living cells are the adult stem/progenitor cells.

Under these conditions, proliferating stem/progenitor cells themselves responded to excitatory stimuli (depolarization or glutamate) with elevations in intracellular Ca^{2+} (measured with the visible Ca^{2+}-sensitive dye X-rhod-1; Fig. 3A,B), indicating expression of responsive Ca^{2+} channels within the proliferating progenitor population. If this intrinsic Ca^{2+} channel activity contributes to neurogenesis, then stimulation of these cells grown on the fixed coculture substrate should still enhance neurogenesis. Consistent with this prediction, the fraction of MAP2ab-positive cells (Fig. 3C) was enhanced by depolarization, to a degree quantitatively comparable to the living coculture. Functional synaptic connectivity between the cells themselves was also enhanced, as evidenced by the increased occurrence of spontaneous synaptic currents (Fig. 3E).

To definitively test whether the Ca^{2+} channels controlling adult excitation-neurogenesis coupling are present on the stem/progenitor population, we applied the specific $Ca_v1.2/1.3$ channel antagonist nifedipine in the fixed-substrate environment. This intervention completely blocked excitation-induced neurogenesis (Fig. 3C). We next made use of the $Ca_v1.2/1.3$ channel agonist FPL 64176 as the only external stimulus and conversely observed an enhancement of neurogenesis (Fig. 3C). We also explored the potential role of NMDA receptors in this controlled fixed-substrate environment and found that NMDA receptor modulation with the antagonist D-AP5 and agonist NMDA likewise bidirectionally modulated neurogenesis (Fig. 3D).

These experiments, in an environment where no other living cells are present, demonstrate that activity-sensing Ca^{2+} channels are present and functioning on adult stem/progenitor cells. Furthermore, despite the lack of excitation-neurogenesis coupling in pure cultures lacking the fixed substrate, we were able to demonstrate that this effect does not depend on indirect activity-dependent signals acting via mature neurons or glia. Proliferating stem/progenitor cells can therefore act as the signal detection and processing elements mediating adult excitation-neurogenesis coupling.

Evaluating potential effects of excitation on proliferation, differentiation, and survival

By design(25), excitation stimuli were applied concurrently with differentiation stimuli to the proliferative stem/progenitor cells to mimic the hypothesized *in vivo* situation, in which proliferating progenitors are exposed to network activity. It remained possible, however, that excitation might also act on cells that have committed to the neural phenotype, by selectively enriching for these committed cells or by altering their post-mitotic differentiation. To further explore whether the excitatory stimuli were sensed by proliferative or post-mitotic cells, we first

established that virtually the entire population of stem/progenitor cells are rapidly proliferating when excitatory stimuli are applied (at the beginning of day 1 after attachment to the fixed substrate). Over 90% of the GFP+ cells were BrdU+ (that is, passing through S-phase of mitosis within the 24 hr labeling period between day 1 and day 2; Fig. 4A). Notably, it is these rapidly proliferating stem/progenitor cells that respond to excitatory stimuli with increased neurogenesis, since even a single brief (5 min) stimulus pulse applied at the beginning of day 1 elicited significant excitation-neurogenesis coupling (Fig. 4B). Similarly, all neurogenic effects were abolished when the anti-mitotic agent FUDR was added after these 5 minutes (or even after an additional 24 hr); under these conditions, more than 95% of all cells were killed, confirming the high mitotic index within cells responding to even brief excitation stimuli (Fig. 4C). Therefore, excitation applied to actively proliferating stem/progenitor cells is sufficient for excitation-neurogenesis coupling.

To determine if proliferation was also necessary for the effects of activity, we delayed application of excitatory stimuli to allow cells to exit the cell cycle under differentiating conditions. Depolarization in the post-mitotic cells had no significant effect on the abundance of new neurons (Fig. 4D). Similarly, delayed application of D-AP5 on day 5 did not prevent excitation-neurogenesis coupling (2.76 ± 0.95-fold neurogenesis enhancement, n=7 independent experiments, versus 2.22 ± 0.25-fold enhancement in control, n=5 experiments; $p>0.5$). We also found that 5 minute spaced pulses of depolarization or the $Ca_v1.2/1.3$ channel agonist FPL 64176 on days 1, 3 and 5 enhanced neurogenesis to a similar extent as continuous excitatory stimulation (Fig. 4B), indicating that even brief bouts of excitation are sufficient to strongly drive excitation-neurogenesis coupling within the proliferative stem/progenitor cell population.

Although Ca^{2+} signaling can in various contexts modulate cell death, proliferation, or survival(31), we found no significant effect of the mild depolarization used here on apoptosis, proliferation, or net survival of these cells at any time point (using TUNEL labeling, BrdU labeling, and total cell counts respectively, Fig. 4E, F). These results do not rule out effects of depolarization on death, survival, or proliferation in other circumstances, but do provide further evidence that the dominant direct effect of excitation on actively proliferating adult stem/progenitor cells is to instructively favor neurogenesis.

Excitation rapidly activates a proneural gene expression program in proliferating progenitors.

To further characterize how excitation drives proliferating stem/progenitor cells to favor the neuronal phenotype, we explored the expression dynamics of transcription factors that influence cell fate decisions by using real-time rtPCR. Specifically, we tracked the expression of the mammalian hairy/Enhancer of split homologs *HES1* and *HES5* (basic helix-loop-helix or bHLH(32) genes which can inhibit neurogeneis and/or promote glial fate)(33), the bHLH gene *Id2* (which also inhibits neuronal fate and differentiation)(34,35), and mammalian acheate-scute homolog-1 *MASH1* (a multifunctional bHLH gene which can either promote or inhibit neuron production (36, 37) and is known to modulate *HES1*/*HES5*(38) expression in proliferating progenitors). In differentiation experiments identical to those in Fig. 3 and Fig. 4, we measured the transcript expression levels of these genes over the first 96 hr following differentiation under a range of conditions, including the presence or absence of excitation, the presence or absence of fixed substrate, and the presence or absence of channel blockers (Fig. 5).

Excitation provoked a rapid, robust and appropriate transcriptional response when applied as usual to the proliferating cells at day 1 after the first 24 hr of substrate attachment. Each gene showed a distinct time course of changes. *HES1* and *HES5* were immediately depressed in the excited sample compared to controls, with a rapid time course beginning within 30 min and proceeding over the first ~24 hr (2 hr to 96 hr shown in Fig. 5A). *Id2* was also inhibited by excitation, albeit with the first clear differences noted at 6 hr (Fig. 5B). Relatively little change was seen in *MASH1* (which has multifunctional roles; Fig. 5B), and little difference was observed after the first 48 hr in any of these genes, indicating that the critical response in these fate-determining genes occurs soon after the initiation of the excitatory stimulation and during the period where virtually all cells are still proliferating (Fig. 4A-C).

We next examined the effects of applying antagonists of $Ca_v1.2/1.3$ Ca^{2+} channels and NMDA receptors and found that conversely this caused a relative *increase* in the expression of these genes (Fig. 5C). Furthermore, these same antagonists largely abolished the changes in gene expression caused by excitation (Fig. 5C). These results demonstrate that the Ca^{2+} influx channels expressed on the rapidly proliferating stem/progenitor cells are functionally coupled to downstream nuclear signaling pathways, and the complex gene expression program initiated by excitation in the proliferating cells is reversed by the same antagonists which block excitation-induced neurogenesis. Importantly, we also found that the usual excitation failed to cause a significant change in gene expression when the cells were plated without the fixed hippocampal substrate (Fig. 5D). These results suggest that the gene expression changes could be a component of the molecular mechanism associated with the need for cellular substrate to elicit excitation-dependent neurogenesis (Fig. 1H).

NeuroD is a downstream master control gene which directly drives expression of an array of genes required for proper mature neuronal functioning, including structural proteins and ion channels, especially in the dentate gyrus(39). Expression of *NeuroD* therefore indicates commitment to the neuronal fate. Though a great number of bHLH genes interact in complex and highly redundant ways to control cell fate(37), if the net outcome of the many fate gene changes caused by excitation (Fig. 5A,B) is to rapidly favor neuronal fate commitment, we would predict that this commitment would be signaled by a relative increase rather than a decrease in expression of *NeuroD* after excitation. Indeed, unlike the glial fate-promoting bHLH genes, *NeuroD* expression was significantly increased by excitation. Strikingly, while excitation-induced changes in the bHLH fate genes were transient, the excitation-induced increase in *NeuroD* expression remained elevated for a more prolonged period (Fig. 5F), befitting a master control gene required for neuronal function. Furthermore, consistent with the excitation-neurogenesis coupling results, this increase was blocked by the Ca^{2+} channel antagonists, and was not present in the absence of fixed hippocampal substrate (Fig. 5E). Together, these data demonstrate that excitation induces a proneural gene expression program in proliferating adult stem/progenitor cells. The rapidity of the gene expression response further demonstrates that no changes in proliferation or survival are necessary to observe the immediate proneural impact of excitation.

***In vivo* control of neurogenesis by $Ca_v1.2/1.3$ channel-specific modulators and activity.**

If this direct excitation-neurogenesis coupling pathway is operative *in vivo* and mediates the effects of physiological electrical activity on neuron production, actively dividing cells would need to exist in a cellular niche that exposes them to network activity. The positioning of the

progenitor cell within the axon-rich environment of the subgranular zone would seem an ideal setting. Indeed, expression of the activity-regulated immediate-early gene (IEG) product Zif-268 (40) within granule layer neurons demonstrates that proliferating progenitor cells are in intimate contact with active neurons (Fig. 6A).

This positioning of neural progenitors within an activity-rich niche suggests that activity-dependent depolarizing mechanisms(41) could directly influence the proliferating progenitor cells, presumably through $Ca_v1.2/1.3$ channels, which do not significantly contribute to synaptic transmission but as noted above serve as a widespread and uniquely potent(27, 28) final common pathway by which electrical signals at the plasma membrane are transduced to the nucleus and give rise to activity-dependent gene expression programs. To test this possibility *in vivo*, we again employed nifedipine as a potent and selective antagonist of the $Ca_v1.2/1.3$ channels, since agents of this class have good CNS penetration. Indeed, we found that *in vivo* administration of nifedipine significantly reduced the fraction of newborn cells assuming the neuronal phenotype ($n=3$; $p<0.001$; Fig. 6B, 6D). We also obtained immunocytochemical evidence for expression of $Ca_v1.2/Ca_v1.3$ channel units *in vivo* in BrdU-positive cells of the hippocampal subgranular zone (not shown). By contrast, direct positive modulation of $Ca_v1.2/1.3$ channels with the agonist FPL 64176 induced a relative increase in the neuronal fraction (Fig. 6C, 6D). These results, in combination with the *in vitro* data, support the hypothesis that $Ca_v1.2/1.3$ channels respond to physiological excitatory activity patterns within local circuits to promote neurogenesis from hippocampal stem/progenitor cells.

The effects of these interventions suggest that $Ca_v1.2/1.3$ channels are activated by normal *in vivo* activity patterns which influence neurogenesis. To test the effects on adult neurogenesis of dampening these activity patterns we examined the consequences of chronic

administration of diazepam, a long-acting benzodiazepine that has been shown to cause a stable, mild reduction in net hippocampal excitatory activity(42). *In vivo* diazepam administration caused a significant reduction in the fraction of BrdU positive cells that assumed a neuronal phenotype without significantly altering the total number of BrdU positive cells (Fig. 6D; n=3; $p<0.002$), providing further evidence that excitatory activity patterns instructively promote adult neurogenesis.

Functional consequences of excitation-neurogenesis coupling

What physiological functions might excitation-neurogenesis coupling in the hippocampus subserve? Current data on the role of neurogenesis within the hippocampus are inconclusive, as adult neurogenesis has been variously implicated in either the storage or clearance of memories(12, 13). Surprisingly, using a simple network modeling approach we find that both views may be correct, as the excitation-neurogenesis coupling relationship described here can, in principle, underlie beneficial effects of adult neurogenesis in *both* memory clearance and memory storage.

Models of information storage using simple simulated neural networks have been used for many years and have deepened our understanding of normal brain functioning(43-46). However, the role of neurogenesis in the functioning of memory-storage neural networks has not been explored (although alterations in sensory information processing in the olfactory bulb have drawn recent attention)(47). Using a simple layered neural network(43) (Fig. 6E) capable of storing and recalling many patterns of activity, we have asked whether new neurons can be usefully incorporated into mature existing networks, and explored the advantages and disadvantages of this process in different activity regimes.

Memories, in the form of patterns of neuronal activity, are stored in the network using associative or Hebbian(45) synaptic plasticity rules like those used in the hippocampus (in this context, "Hebbian" simply means that when two neurons are active at the same time during exposure to an input, the efficacy of the synaptic connection between them is increased). Apart from this hippocampus-like provision, no detailed assumptions about wiring or dynamics were made, as little is known about the functional relevance of these parameters to how information is actually stored in the brain. The network has a simple three-layered structure (Fig. 6E, 6F) and robustly stores many memories in the form of activity patterns in the third (output) layer. Appropriately patterned output (i.e., memory recall) is elicited by patterned stimulation of the first (input) layer. Simple networks such as these have been widely used as models for information processing or memory storage (43-46).

We compared the function of a control, stable network to a network in which neurogenesis occurs in only the middle layer (as thought to occur *in vivo* in the dentate gyrus; steady addition of new neurons was balanced by steady loss of existing neurons, keeping network size unchanged). We observed two key network behaviors relating to memory clearance and memory storage. First, we found that neurogenesis elicited a more rapid loss or clearance of previously stored old memories (Fig. 6G). To some extent this may be expected, as the synapses of the new neurons have no access to information on the old memories formed before their birth, and the behavior of the new neurons therefore cannot help and can only degrade the network's ability to recall old memories. This aspect of the model may provide a quantitative framework for understanding how a balance of neuron loss and replacement could be important for clearance of previously stored memories(13).

Secondly, with regard to storage of new memories, we found that the newest memories were recalled at a higher fidelity (compared to the zero-neurogenesis stable case) when neurogenesis was allowed to occur (Fig. 6H), despite the fact that total network size was not allowed to increase. This effect can be intuitively understood from the lack of involvement of new neurons in old memories; in effect, their synapses can be devoted more fully to the newer memories, which are then more accurately stored. Critically, this advantage was dramatically greater in networks that had been more active and had been required to store many memories, by comparison with the low activity (low storage rate) networks. This conditional advantage of neurogenesis for memory storage and recall predicts a monotonically increasing function linking network activity level to the relative benefits of neurogenesis in memory storage (Fig. 6H).

Such a relationship was in fact found experimentally in the excitation-neurogenesis coupling characteristics of the adult stem/progenitor cells (Fig. 6I). Because both NMDA receptors and $Ca_v1.2/1.3$ Ca^{2+} channels mediate their long-lasting effects through Ca^{2+} flux, we tested the dependence of neurogenesis on Ca^{2+} by varying external $[Ca^{2+}]$ in the setting of depolarization in the fixed coculture substrate condition (Fig. 6I). As external $[Ca^{2+}]$ was increased over a broad range up to 1.8 mM, neurogenesis monotonically increased, indicating that within this range a monotonic relationship with positive slope exists between external Ca^{2+} and the extent of neurogenesis. Since there were no living cells present except for the stem/progenitor cells, these experiments demonstrate that processing mechanisms within the stem/progenitor cells themselves can implement the simple rules governing the excitation-neurogenesis coupling that had been predicted from network modeling.

Discussion

Using an array of approaches, we have explored the coupling of excitation to neurogenesis in proliferating adult-derived stem/progenitor cells, both *in vitro* and *in vivo*. Neurogenesis is greatly enhanced by excitatory stimuli, and involves $Ca_v1.2/1.3$ channels and NMDA receptors. Surprisingly, despite a clear requirement for the appropriate microenvironment in this process(23) (Fig. 1H), channels located directly on the proliferating stem/progenitor cells sense and process excitatory stimuli, subsequently transmitting signals to the nucleus for rapid induction of a proneural gene expression program. The resulting cells become fully functional neurons, as determined by expression of neuronal proteins and synaptic incorporation into active neural circuits. In addition, several important characteristics of this process were identified, including that brief pulses of excitation can be sufficient to drive neurogenesis, and that a monotonically increasing function characterizes excitation-neurogenesis coupling. Finally, incorporation of this form of excitation-neurogenesis coupling into a layered neural network suggests surprisingly clear advantages for *both* the clearance of old memories and the storage of new memories. Taken together, these results provide a new experimental and theoretical framework for further investigation of adult excitation-neurogenesis coupling.

Previous studies have reported activity-dependent proliferative bursts in the dentate gyrus subgranular zone caused by a multitude of different interventions (1, 8, 14, 15, 18, 19, 21). Here we provide specific mechanisms that may underlie control of the neurogenesis observed after such proliferative bursts, particularly in those cases in which excitatory activity is present in the ensuing days (e.g. after stroke, seizure, or electrical stimulation). The observation that brief NMDA receptor blockade induced robust stem/progenitor cell proliferation(21) might seem conceptually in conflict with the present results which demonstrate that stimulation of NMDA receptors increases neurogenesis. In fact, the two sets of results are particularly compatible since

after clearance of the antagonist, neuronal activity would presumably return to appropriate levels, allowing excitation during proliferation to promote neuronal fate selection. Indeed, it has been reported that most of the new cells produced following brief NMDA receptor blockade become neurons(21). Such a mechanism may be particularly appropriate in light of the fact that excess glutamate leading to NMDA receptor activity can be toxic to mature neurons; linking the same excess glutamate to the production of new neurons would presumably be of adaptive value for the organism.

That excitation of adult stem/progenitor cells promotes neurogenesis separately from proliferative or apoptotic selection has important clinical implications(17), particularly as stem/progenitor cells have been shown to invade regions of damaged brain tissue following stroke(1, 48), and in some circumstances can contribute to long-range connections and functional recovery(1, 16). It is conceivable that pharmacological interventions or manipulations of neural activity could enhance the ability of either native or transplanted progenitor cells to restore function to damaged areas of the CNS. Electroconvulsive stimulation and seizures promote generation of new cells in the dentate gyrus of the hippocampus(14, 15, 18), and electroconvulsive therapy (ECT) as used for treatment of psychiatric and neurological disorders involves brief (~1 min) pulses of excitatory activity provided every other day. This therapeutic pattern is similar to the pulse pattern provided in Fig. 4B, suggesting that ECT could be adapted to specifically promote neurogenesis. It will be important to conduct further mechanistic work in reduced preparations to identify specific ways by which these cells might be manipulated to promote further their incorporation into neural circuits in damaged areas *in vivo*.

Adult excitation-neurogenesis coupling could also be a special adaptation with a unique information processing purpose. In the model neural network, this single phenomenon

surprisingly promoted both clearance of old memories and storage of new memories, precisely the two roles to which adult neurogenesis has been experimentally linked(12, 13). Indeed, certain of the molecular players shown here to be important for excitation-neurogenesis coupling (e.g. NMDA receptors) are also known to be important for stable memory formation in mammals(30). The existence of excitation-neurogenesis coupling may be particularly important in the hippocampus, a heavily-used locus for temporary memory storage(49), where rapid memory turnover heightens the need for efficient means of eliminating old memories while reliably storing new memories. Ideally progenitors would be able to distinguish activity relating to new memory storage (which should trigger neurogenesis) from activity relating only to use of old memories (which should not necessarily lead to a requirement for more neurons as there is not increasing memory load placed on the circuits). Therefore adult excitation-neurogenesis coupling need not be a constitutive property of stem/progenitor cells, but may exist in modes which can be switched on or off by the specific signatures of the modulatory inputs.

Likewise, not every neurogenic region in the brain need follow the excitation-neurogenesis coupling rule outlined here; rather, an activity rule appropriate for the unique information-processing or storage function of that brain region might be expected to operate. In this context it is interesting to note that olfactory bulb precursor neurogenesis (in contrast to hippocampal neurogenesis) is not enhanced by behavioral activity(50), but proliferation and survival can be influenced by sensory stimuli(51), suggesting that a different activity rule may govern olfactory bulb neurogenesis. Cells with neurogenic potential are present in additional areas of the adult brain, including neocortex (52), but contribute to neurogenesis only in the subventricular zone and the dentate gyrus subgranular zone. However, when cells from non-neurogenic areas are removed and transplanted into neurogenic areas, neuronal progeny

result(52). Our findings are consistent with the principle that local cellular environments are important in controlling neurogenesis, and in particular with the recent demonstration that hippocampal coculture promotes hippocampal neurogenesis(23). Importantly, our findings extend these observations by demonstrating novel rules that govern neurogenesis. In addition to the role played by the region-specific identity of astroglia(23), our results suggest that one contributing factor to the different neurogenic potential of different brain areas may be differences in local neuronal activity. These key differences may in turn be superimposed upon subtle local differences in neurogenic potential of the progenitors themselves, although we currently lack specific cellular markers to sort out these subtle heterogeneities. Indeed, by all accounts different stem/progenitor cell populations *in vivo* as well as *in vitro* vary with regard to lineage potential and therefore may be heterogeneous with regard to functional potential as well. That the neurons generated as a consequence of excitation are synaptically coupled underscores the importance of further elucidating the detailed rules governing the activity-dependent incorporation of new neurons into functional neural networks.

Figure legends

Figure 1. Adult excitation-neurogenesis coupling.

A, HC37 cells cultured alone reveal little neurogenesis, based on morphology and MAP2ab expression. Left column, GFP+ cells. Right column, overlay of GFP (green) and MAP2ab (red) expression, with spatial overlap (yellow) signifying the conjunction. **B**, HC37 cells grown with hippocampal neurons and glia assume neuronal morphology and express high levels of MAP2ab. **C**, Coculture resulted in a 2.6-fold increase in the fraction of cells assuming a neuronal fate ($p<0.05$; n=4 experiments). The fraction of GFP+ cells that were MAP2ab+ is normalized to the fraction found in the –coculture condition. Mean neuron fraction in the control coculture case across all experiments was 23%. **D**, Example of whole-cell patch clamp recording from a stem/progenitor cell-derived neuron in coculture. **E**, Example of voltage-activated Na^+ current evoked from a stem/progenitor cell-derived neuron. Tetrodotoxin (TTX, 1 μM) reversibly blocked the inward current evoked with a step from –70 mV to –10 mV. **F**, As with MAP2ab expression, mixed hippocampal coculture consistently increased expression of Na^+ current ($p<0.01$, n=22 cells for –coculture and n =26 cells for +coculture; pooled data from 2 independent experiments). **G**, Quantitative assessment of morphological development and association with MAP2ab expression. Glial-type cells without primary processes (0-1; e.g. astroglial) or with very high numbers of primary processes (>14; e.g. oligodendroglial) consistently expressed little MAP2ab, regardless of culture conditions, indicating that coculture does not exert a nonspecific effect on MAP2ab expression. Neuronal cells, morphologically defined as cells having a small number (2-5) of well-defined primary processes, expressed high levels of MAP2ab. **H**, Effects of excitatory stimuli: depolarization (K; n=12 independent

experiments; $p<0.01$) strongly elevated the fraction of neurons among the stem cell progeny. The fraction of GFP+ cells that were MAP2ab+ is normalized to the fraction found in the Na condition. Absence of surrounding hippocampal tissue (-coculture) impairs not only basal neurogenesis but also the ability to respond to depolarization stimuli with increased neurogenesis (pooled data from 3 independent experiments). **I**, Excitation increases neurogenesis, not extent of neuronal differentiation, in individual cells. Shown is MAP2ab intensity vs. frequency histogram of cells in control (Na) or depolarized (K) conditions from a representative experiment. Excitatory activity did not simply promote progression through differentiation after fate commitment, as depolarization increased the proportion of cells expressing high levels of MAP2ab without generating cells that expressed MAP2ab at unusually high levels (histogram).

Figure 2. Characteristics of stem/progenitor cell-derived neurons induced by excitation and requirement for Ca^{2+} channels.

A, Excitatory neurotransmitter application (Glu; n=6 independent experiments; $p<0.05$) also promotes neurogenesis; depolarization effect (K) shown again for comparison (black bars). Also shown is summary data on extent of single-cell neuronal differentiation in control and excitation conditions as measured by MAP2a,b expression level (gray bars). There was no effect of either stimulus on the mean MAP2ab intensity in the resulting neuronal progeny ($p=0.21$ for K, $p=0.40$ for Glu) or in the non-neuronal progeny (not shown), indicating that activity increases neuron production rather than extent of neuronal differentiation. Likewise in those (neuronal) cells with TTX-sensitive voltage-gated sodium channel currents, current density was not altered by depolarization (not shown). **B**, Analysis of the neuronal marker Doublecortin (Dcx) also revealed a marked excitation-dependent increase. Left: Dcx staining in adult rat dentate gyrus,

demonstrating that only young neurons express this early marker, namely those neurons still lining the subgranular zone and sending processes into the granule cell layer (bracket). Right: Dcx staining *in vitro*, in the control (Na) or excitation (K) condition; conducted under the same experimental conditions as the MAP2ab assay. **C**, The excitation-induced increases in MAP2ab and Dcx, two structurally and functionally distinct neuronal proteins, are highly correlated at the single-cell level (n=304; $r^2 = 0.4654$; $p < 0.0001$), supporting the identification of these cells as neurons. **D**, Excitation increased the fraction of cells with functional excitatory synapses as defined by the occurrence of miniature EPSCs. Sample traces from the control (Na) condition (upper trace) and following glutamate stimulation (lower trace) are shown on the right. **E**, The $Ca_v1.2/1.3$ antagonist nifedipine inhibited basal and excitation-induced neurogenesis (n=3 experiments per condition). Drugs were provided with the differentiation medium in conjunction with the stimuli. **F**, Inhibition of NMDA receptors with D-AP5 (50 μM) also blocked excitation-induced neurogenesis, via either depolarization or glutamate application. Depolarization (K), n=6 experiments; $p<0.05$; glutamate (Glu), n=3 experiments; $p= 0.05$.

Figure 3. Proliferating adult hippocampal stem/progenitor cells directly sense excitation and respond with increased neurogenesis.

A, Depolarization with KCl causes elevations of $[Ca^{2+}]_i$ in proliferating adult-derived stem/progenitor cells grown on a fixed substrate of hippocampal cultures. Shown is x-Rhod-1 fluorescence expressed as F/F_0; increased fluorescence demonstrates elevated $[Ca^{2+}]_i$ which is superimposed on slow photobleaching of the indicator. Mean values of all loaded cells are shown (n=50 cells). Pseudocolor images of the field of cells are shown in the inset at timepoints corresponding to *a* and *b*. Warmer (longer wavelength) colors correspond to higher levels of

$[Ca^{2+}]_i$. **B**, Adult-derived stem/progenitor cells express functional NMDA receptors. $[Ca^{2+}]_i$ response to applied glutamate measured with x-Rhod-1 (n=73) is blocked by 50 μM AP5/10 μM MK-801 (n=17). **C**, Adult-derived stem/progenitor cells cultured on a fixed hippocampal substrate display robust excitation-neurogenesis coupling (n=7 independent experiments). Bidirectional changes in neurogenesis result from application of $Ca_v1.2/1.3$ channel agonist (FPL64176, 5 μM) or antagonist (nifedipine, 10 μM). **D**, Bidirectional changes in neurogenesis also result from application of NMDA receptor agonist (NMDA, 50 μM) or antagonist (D-AP5, 50 μM). **E**, Excitation enhances frequency of synaptic connectivity between stem/progenitor cells plated on the fixed hippocampal substrate or with conditioned medium from hippocampal cells (light fixation: 0/23 Na, 4/17 K; hippocampal conditioned medium: 0/12 Na, 2/12 K). Traces on the right show sample mEPSCs.

Figure 4. Assessment of proliferation, survival, and differentiation.

A, Example of BrdU-labeled cells indicating that excitatory stimuli are applied to proliferating cells; >90% of the stem/progenitor cells were BrdU+ after a 24 hr label beginning on day 1. It does not appear that even a tiny fraction of the stem/progenitor cells become postmitotic neurons during the initial day of substrate attachment in mitogens; in a separate experiment, when cells were plated as usual on the lightly fixed substrate with the mitogens, but in the absence of usual subsequent differentiation factors, neurons were clearly not generated as no observed cells in this condition demonstrated MAP2 positivity even by 14 days (not shown). **B**, Brief, spaced excitatory stimuli robustly enhance neurogenesis. When given as a single 5 min pulse on day 1, direct depolarization of the proliferating cells was sufficient for significant excitation-neurogenesis coupling (n=5; $p<0.05$). Three 5 min pulses spaced every other day (day 1, 3, and 5

after substrate plating and proliferative stimulation) were also effective when given as depolarization (K), direct $Ca_v1.2/1.3$ channel activation with FPL 64176 (FPL), or the combination (K/FPL). **C**, Confirming that this stimulus is received by proliferating progenitors, application of the anti-mitotic agent FUDR led to >95% cell death when given immediately after the initial 5 min on day 1, or even after an additional 24 hr. **D**, Excitation applied to postmitotic cells does not give rise to excitation-neurogenesis coupling; depolarization was initiated after full cell-cyle withdrawal on day 6, 8, or 10 and phenotype was assayed on day 14 (n=3; p>0.2 for all 3 conditions). **E**, Assessment of proliferation, survival, and differentiation during days 2 and 3 (average) in excitation or control conditions. Neuronal fraction is defined as the mean MAP2ab+ fraction. Proliferative fraction is defined as the mean BrdU+ fraction after a 2 hr BrdU labeling period and immediate fixation. Apoptosis index is defined as the mean total TUNEL+ cells observed per 20 random fields. Mean of 3 independent experiments in pure stem/progenitor cells growing on fixed substrate. all +/- SEM. Note that MAP2 positive cells are virtually absent within the first 2 days, consistent with the proliferation data in A-C and demonstrating the absence of differentiated neurons; notably, it is within this 48 hour period that Ca^{2+} imaging was performed (Fig. 3A,B). **F**, Assessment of proliferation, survival, and differentiation during days 8 and 9 in excitation or control conditions, as in E. Total cell counts from 20 random fields between day 8 and 9 yielded 52±18 cells in the control condition and 48±7.7 cells in the excitation condition, obtained from three independent experiments; p=0.84; not shown). Total cell count is defined as the mean total GFP+ cells per 20 random 40x microscope fields.

Figure 5. Gene expression profiles underlying excitation-neurogenesis coupling in adult stem/progenitor cells.

A, Immediate bHLH gene response to excitation. Proliferating stem/progenitors were stimulated at the usual time (1 day after plating on fixed substrate in mitogens) along with the usual differentiation factors. Excitation (K) was supplemented with FPL64176 as in Fig. 3C. *HES1* and *HES5* (glial fate promoting genes) showed a markedly inhibited profile over the first 1-2 days in the excited samples. All values were normalized to GAPDH transcript levels. Each sample was tested in five replicates, and similar results were observed in three independent experiments. Responses could be detected as early as 30 min (not shown); values shown are percent of initial (t=0) values. **B,** *Id2* likewise showed a strong inhibition by excitation, although first effects were not clearly apparent until 6 hr, while *MASH1* was generally driven to low levels by the differentiation factors. **C,** Comparison of the 6 hr timepoint for all bHLH genes with effects of calcium channel influx antagonists. Dashed line corresponds to the unstimulated (Na)/no drug condition for each gene. AP5/nifedipine treatment drives gene expression in the opposite direction as excitation (compare with the marked reductions in the glial fate genes seen at 6 hr in Fig. 5A, 5B), and furthermore blocks excitation-induced changes in the bHLH genes. **D,** Comparison of the 6 hr timepoint for bHLH genes, after plating on the standard polyornithin/laminin susbtrate instead of the lightly fixed hippocampal susbtrate. Dashed line corresponds to unstimulated (Na) condition for each gene; plotted values are in the excitation condition. No excitation-induced inhibition of glial fate genes was observed. **E**, *NeuroD* expression was increased by excitation; the increase was blocked by the channel antagonists and not seen in the absence of substrate. **F**, Time course of *NeuroD* expression reveals a persistent elevation caused by excitation.

Figure 6. Excitation-neurogenesis coupling in intact neural netwoks.

A, Cellular niche occupied by adult hippocampal progenitors *in vivo*: IEG activation and cell proliferation. Representative triple staining for BrdU, Doublecortin (Dcx) and Zif-268 in adult hippocampal slices, with colors used indicated below the image. Bracket marks dentate gyrus granule cell layer in panels A-C; all are confocal micrographs, 40x magnification, zoom of 4. **B**, Modulation of $Ca_v1.2/1.3$ channels *in vivo* significantly influences neurogenesis. For 1 week, adult rats received daily injections of BrdU (50 mg/kg) and either vehicle, nifedipine, FPL 64176, or diazepam (all at 4 mg/kg) as indicated, followed by perfusion and staining for Dcx (red) and BrdU (green); conjunction of the two is shown as yellow. Phenotype of newborn cells was assessed by confocal microscopy with full z-axis analysis. Total numbers of BrdU+ cells were comparable in all conditions; representative image from the nifedipine condition shown. **C**, Representative image from the FPL 64176 condition shown. **D**, Summary graph of Ca^{2+} channel modulation results. 3 adult female rats were used per condition, with plotted values normalized to control neuronal fraction of 35.3% and representing the fraction of cells among those proliferating during the experimental period (BrdU+) which came to express the early neuronal phenotype (Dcx+). **E**, Diagram of modified associative neural network based on the Willshaw model(43), with simple parallels to hippocampal processing. Key characteristics are its 3-layered structure, feedforward connectivity, sparse representations, and memory storage capability via use of Hebbian synapses (see methods). **F**, Memories are presented to the input layer (layer 1), processed by the middle layer (layer 2, where neurogenesis is also allowed to occur), and performance assessed at the output layer (layer 3). Performance is quantified as the Hamming distance, defined as the number of output units at which the actual output pattern differs from the learned one. Note the output layer neuron that is incorrectly inactive (*), which would lead to a Hamming distance score of 1. **G**, Memory loss/clearance caused by cell turnover (balanced

neurogenesis and cell death at the hidden layer only; this corresponds to the apparent limitation of adult neurogenesis to the dentate gyrus layer in mammalian hippocampus in nonpathological situations). Older memories are gradually degraded and lost (seen as increased Hamming distance) as the network stores new memories with the Hebb rule. Although even without turnover (stable case) old memories are increasingly lost as new memories are stored, memory loss/clearance is greatly accelerated by the presence of balanced neurogenesis and cell death (neurogenesis case). Here each unit of "time post-learning" correspond to the learning of 50 new memories; significant degradation of old memories seen even in the stable case begins to be apparent after time=6 (shown) corresponding to 300 stored patterns in a network of 500 neurons per layer. **H**, Marked advantage in storing new memories by allowing neurogenesis/turnover to occur in an excitation-induced manner. High-activity networks involved in high rates of pattern storage increasingly (and monotonically) benefit from turnover. New neurons are better suited to handle incoming memories because of their lack of synaptic involvement in old memories. Network activity level is measured again in units of 50 stored patterns, with higher levels of pattern storage corresponding to more active networks. Mean values shown in bar plots represent Hamming distances averaged over all stored patterns. **I**, Experimentally determined neurogenesis increases as a monotonic function of extracellular Ca^{2+}. Steady depolarization was provided in the presence of 20 mM K^+, and varying $[Ca^{2+}]_o$; mean data from 3 independent experiments shown performed in cells plated on a fixed hippocampal substrate.

References

1. A. Arvidsson, Z. Kokaia, O. Lindvall, *Eur J Neurosci* **14**, 10-8. (2001).
2. B. S. McEwen, *Ann N Y Acad Sci* **746**, 134-42; discussion 142-4, 178-9. (1994).
3. H. A. Cameron, R. McKay, *Curr Opin Neurobiol* **8**, 677-80. (1998).
4. P. Taupin, F. H. Gage, *J Neurosci Res* **69**, 745-9. (2002).
5. U. Maskos, O. Brustle, R. D. McKay, *Dev Biol* **231**, 103-12. (2001).
6. M. Verhage *et al.*, *Science* **287**, 864-9. (2000).
7. E. Y. Snyder, C. Yoon, J. D. Flax, J. D. Macklis, *Proc Natl Acad Sci U S A* **94**, 11663-8. (1997).
8. E. Gould, P. Tanapat, T. Rydel, N. Hastings, *Biol Psychiatry* **48**, 715-20. (2000).
9. A. Alvarez-Buylla, B. Seri, F. Doetsch, *Brain Res Bull* **57**, 751-8. (2002).
10. R. M. Seaberg, D. van der Kooy, *J Neurosci* **22**, 1784-93. (2002).
11. S. Temple, *Nature* **414**, 112-7. (2001).
12. T. J. Shors *et al.*, *Nature* **410**, 372-6. (2001).
13. R. Feng *et al.*, *Neuron* **32**, 911-26. (2001).
14. J. M. Parent *et al.*, *J Neurosci* **17**, 3727-38. (1997).
15. J. E. Malberg, A. J. Eisch, E. J. Nestler, R. S. Duman, *J Neurosci* **20**, 9104-10. (2000).
16. E. Y. Snyder, A. L. Vescovi, *Nat Biotechnol* **18**, 827-8. (2000).
17. A. Bjorklund, O. Lindvall, *Nat Neurosci* **3**, 537-44. (2000).
18. T. M. Madsen *et al.*, *Biol Psychiatry* **47**, 1043-9. (2000).
19. J. Liu, K. Solway, R. O. Messing, F. R. Sharp, *J Neurosci* **18**, 7768-78. (1998).
20. H. van Praag, B. R. Christie, T. J. Sejnowski, F. H. Gage, *Proc Natl Acad Sci U S A* **96**, 13427-31. (1999).
21. H. A. Cameron, B. S. McEwen, E. Gould, *J Neurosci* **15**, 4687-92. (1995).
22. T. D. Palmer, J. Takahashi, F. H. Gage, *Mol Cell Neurosci* **8**, 389-404 (1997).
23. H. Song, C. F. Stevens, F. H. Gage, *Nature* **417**, 39-44. (2002).
24. M. L. Monje, S. Mizumatsu, J. R. Fike, T. D. Palmer, *Nat Med* **5**, 5 (2002).
25. Materials and methods are available as supporting material on Science Online.
26. J. Nacher, C. Crespo, B. S. McEwen, *Eur J Neurosci* **14**, 629-44. (2001).
27. A. E. West *et al.*, *Proc Natl Acad Sci U S A* **98**, 11024-31. (2001).
28. K. Deisseroth, E. K. Heist, R. W. Tsien, *Nature* **392**, 198-202. (1998).
29. R. C. Malenka, R. A. Nicoll, *Science* **285**, 1870-4. (1999).
30. M. F. Bear, R. C. Malenka, *Curr Opin Neurobiol* **4**, 389-99. (1994).
31. Z. Mao, A. Bonni, F. Xia, M. Nadal-Vicens, M. E. Greenberg, *Science* **286**, 785-90. (1999).
32. R. Kageyama, S. Nakanishi, *Curr Opin Genet Dev* **7**, 659-65. (1997).
33. K. Tanigaki *et al.*, *Neuron* **29**, 45-55. (2001).
34. S. Wang, A. Sdrulla, J. E. Johnson, Y. Yokota, B. A. Barres, *Neuron* **29**, 603-14. (2001).
35. J. G. Toma, H. El-Bizri, F. Barnabe-Heider, R. Aloyz, F. D. Miller, *J Neurosci* **20**, 7648-56. (2000).
36. L. Cai, E. M. Morrow, C. L. Cepko, *Development* **127**, 3021-30. (2000).
37. E. Cau, G. Gradwohl, S. Casarosa, R. Kageyama, F. Guillemot, *Development* **127**, 2323-32. (2000).
38. E. Cau, S. Casarosa, F. Guillemot, *Development* **129**, 1871-80. (2002).
39. M. H. Schwab *et al.*, *J Neurosci* **20**, 3714-24. (2000).

40. P. J. French *et al.*, *Eur J Neurosci* **13**, 968-76. (2001).
41. J. G. Jefferys, *Physiol Rev* **75**, 689-723. (1995).
42. V. G. Longo, M. Massotti, D. DeMedici, A. Valerio, *Pharmacol Biochem Behav* **29**, 785-90. (1988).
43. B. Graham, D. Willshaw, *Neural Comput* **11**, 117-37. (1999).
44. J. J. Hopfield, D. W. Tank, *Science* **233**, 625-33. (1986).
45. T. J. Sejnowski, *Neuron* **24**, 773-6. (1999).
46. J. L. McClelland, D. E. Rumelhart, *J Exp Psychol Gen* **114**, 159-97. (1985).
47. L. Petreanu, A. Alvarez-Buylla, *J Neurosci* **22**, 6106-13. (2002).
48. H. Nakatomi *et al.*, *Cell* **110**, 429. (2002).
49. L. R. Squire, S. Zola-Morgan, *Science* **253**, 1380-6. (1991).
50. Brown J, Kempermann G, Van Praag H, Winkler J, Gage FH, Kuhn HG., *European Journal of Neuroscience* **17**, 2042-2046 (2003).
51. C. Rochefort, G. Gheusi, J. D. Vincent, P. M. Lledo, *J Neurosci* **22**, 2679-89. (2002).
52. T. D. Palmer, E. A. Markakis, A. R. Willhoite, F. Safar, F. H. Gage, *J Neurosci* **19**, 8487-97. (1999).
53. We acknowledge support of the Medical Scientist Training Program (S.S.), the Stanford Department of Neurosurgery (H.T., M.M., T.D.P.), grants from the NIH (R.C.M), and helpful discussions with Xiang Yu, Mark Schnitzer, and Eric Wexler. We are also grateful to Greer Murphy, Olivera Mitrisinovic, and William Ju for valuable assistance with experiments.

Supporting Online Material

www.sciencemag.org

Materials and Methods
Supporting references and notes

Supporting Online Material

Methods

In vivo neurogenesis assays

For *in vivo* manipulation of neurogenesis, adult 160g female Fisher rats were injected once per day over a six day period with BrdU (50 mg/kg i.p. in 0.9% saline) along with drug or vehicle control (1% Tween-80/1% ethanol; drug and vehicle injections were over 7 days, initiated one day before the BrdU injections commenced), anaesthetized (0.75 mg/kg acepromazine, 80 mg/kg ketamine and 20 mg/kg xylazine in saline), and sacrificed on the 7th day after BrdU initiation by transcardial perfusion with chilled 4% paraformaldehyde in PBS, followed by overnight postfixation via submersion in 4% PFA/PBS. The agents used (FPL 64176, nifedipine, and diazepam) are highly hydrophobic and chosen to cross the blood-brain barrier, necessitating the use of vehicles for solubilization in the injection; the fraction of BrdU+ cells also staining with Dcx (control case~ 35%) was lower than in previous experiments (Monje et al., 2002; this is likely due to the vehicles, as parallel experiments with normal saline vehicle showed ~85% double-labeling. Over this timescale neither vehicle agent has yet been shown to affect neurogenesis in the hippocampus). FPL 64176, nifedipine, and diazepam were all dosed at 4 mg/kg in an injection volume of 1.6 ml, diluted from 50x stocks. All treatments were well-tolerated with the exception of FPL 64176, as previously reported (Jinnah et al., 2000). Although the low dose used did not lead to overt dystonias, two of the FPL 64176-treated animals died shortly before sacrifice on the 7th experimental day. The brains of these two animals were removed and coronally sliced to expose the hippocampus; fixation by 4% PFA/PBS submersion

overnight and subsequent staining was quantitatively indistinguishable from the FPL 64176/transcardially perfused condition.

For $Ca_v1.2$/$Ca_v1.3$ channel staining *in vivo*, adult 160g female Fisher rats were injected with BrdU (50 mg/kg i.p. in 0.9% saline, every 2 hours, 3 injections) then immediately anaesthetized, transcardially perfused and fixed as above. 40 μm sections were prepared and immunostained according to published protocols. Rabbit anti-α_1C ($Ca_v1.2$) and anti-α_1D ($Ca_v1.3$) were obtained from Alomone Laboratories and used at 1:500; confocal images were obtained and Z-series imaging and projections were employed to ensure correct identification of cells. As expected, very few BrdU+ cells were observed in this assay period (use of a brief labeling period was necessary in order to identify actively dividing cells, rather than cells which simply had been dividing at some point in the past and were now expressing these channels), and only low-level channel staining was observed even in the mature neurons in the intact tissue.

Following fixation, brains were immersed in 30% sucrose/dH_20 for 4 days; 40 μM sections were cut and stored in HistoPrep cryoprotectant prior to staining. Floating sections were rinsed in TBS followed by block for 30 min in 0.3% Triton X-100 and 3% Normal Donkey Serum in TBS (TBS++). Primary antibody staining was conducted in TBS/ 1% Normal Donkey Serum/0.3% Triton X-100 overnight at 4 degrees C on a rotary shaker. Primary antibodies used were goat anti-Doublecortin (1:500, Santa Cruz Biotechnology), rat anti- BrdU (1:500, Accurate), and rabbit anti-Egr-1 (also known as zif-268; 1:200, Oncogene). Sections were then rinsed 3x in TBS, followed by overnight incubation in fluorophore-conjugated secondary antibody (1:1000) staining in TBS++. Sections were again rinsed 3x in TBS and postfixed for 10 min at room temperature in 4% PFA/PBS, rinsed 1x in 0.9% saline, denatured for 30 min at 37 degrees in 2 M HCl, rinsed in TBS, blocked and stained as above for BrdU, aligned on slides in

50 mM phosphate buffer, partially dried, mounted, and coverslipped in 125 mL polyvinyl alcohol-DABCO.

Adult neural stem cell line derivation and culture

Adult hippocampus-derived neural stem/progenitor cells were isolated from adult rat hippocampi and cultured as previously described (Palmer et al., 1997). Briefly, adult female Fisher-344 rats were deeply anesthetized with sodium pentobarbital and were dissected immediately. Hippocampi were enzymatically dissociated with papain (2.5 U/ml; Worthington, Freehold, NJ)-dispase II (1U/ml; Boehringer Mannheim, Indianapolis, IN)-DNase I (250U/ml, Worthington) solution. Digested tissue was then washed with DMEM-10% fetal calf serum (FCS) and subsequently mixed with PBS-equilibrated Percoll solution to a final concentration of 35% Percoll. The Percoll solution was made by mixing nine parts of Percoll (Amersham Pharmacia Biotech, Uppsala, Sweden) with one part of 10× PBS. The cell suspension was then fractionated by centrifugation for 10 min at 1000 × *g*. Floating myelin and tissue debris were discarded and the cell pellet re-suspended in 65% Percoll solution and fractionated again by centrifugation for 10 min at 1000 x *g*. The floating neural progenitors were collected, washed free of Percoll, and plated onto poly-L-ornithine/laminin-coated dishes in DMEM/F12 (1:1) containing 10% FCS medium for 24 hrs; then medium was replaced with serum-free growth medium consisting of DMEM/F12 (1:1) supplemented with N2 supplement (Invitrogen, Gaithersburg, MD) and 20 ng/ml of human recombinant FGF-2 (Peprotech, Rocky Hill, NJ). Cell lines were labeled via infection with replication deficient GFP-expressing recombinant retrovirus, NIT-GFP (Palmer et al., 1999) or LZRS-CAMut4GFP(Okada et al., 1999). HC37 cells transduced with NIT-GFP were used at passage number 25 to 30. Cell lines were propagated in DMEM/F12 with 20 ng/ml

bFGF, penicillin/ streptomycin/ amphotericin B (Life Technologies), and N2 supplement (Life Technologies). Plastic tissue culture-treated dishes were coated with 10 μg/ml polyornithine in dH_20 overnight under UV illumination, rinsed 2x with dH_20, recoated with 5 μg/ml mouse laminin (Invitrogen), incubated overnight at 37ºC, and frozen for long-term storage at –80ºC. Cells were fed every 2-3 days by 75% solution exchange and split 1:4 every 6-7 days after brief trypsinization and centrifugation. Freezing was in DMEM/F12/10% DMSO/BIT supplement (StemCell Technologies), and thawing from storage was in DMEM/F12/BIT.

Hippocampal cell culture

Hippocampi of postnatal day 0 (P0) Sprague-Dawley rats were removed and placed in a dissecting solution containing (in mM): 161 NaCl, 5.0 KCl, 2.9 $CaCl_2$, 5.0 HEPES, and 5.5 glucose, 0.53 $MgSO_4$, and 0.0056 phenol red, pH 7.4. Tissue was treated with papain (20 U/ml) in 10 ml of this solution with additional (in mM) 1.7 cysteine, 1 $CaCl_2$, and 0.5 EDTA for 45 min at 37°C. The digestion was stopped by replacing the solution with 10 ml of MEM/Earle's salts without L-glutamine along with 20 mM glucose, Serum Extender (1:1000), and 10% heat-inactivated fetal bovine serum containing 25 mg of bovine serum albumin (BSA) and 25 mg of trypsin inhibitor. The tissue was triturated in a small volume of this solution with a fire-polished Pasteur pipette, and ~100,000 cells in 1 mL plated per coverslip in 24-well plates. Glass coverslips (pre-washed overnight in HCl followed by several 100% EtOH washes and flame sterilization) were coated overnight at 37ºC with 1:50 Matrigel (Collaborative Biomedical Products, Bedford, MA). Cells were plated in culture medium, Neurobasal containing 2x B-27 (Life Technologies) and 2 mM Glutamax-I (Life Technologies). One-half of the medium was replaced with culture medium the next day, giving a final serum concentration of 1.75%. For

lightly fixed tissue experiments, stem/progenitor cells were plated after hippocampal cultures at 7 DIV were exposed to 70% EtOH at –20ºC for 30 min, then washed 2x in sterile PBS. The stem/progenitor cells were plated on the fixed substrate in 25% conditioned medium from the neuron/glia culture and 75% culture medium, as in coculture experiments (see below).

Stem cell coculture

75% of the medium was removed from each well of the hippocampal cultures and replaced with Neurobasal/B27/ penicillin/streptomycin/glutamine (coculture solution) containing the additional mitogens 20 ng/ml VEGF and 20 ng/ml PDGF (both from Peprotech) and rapidly proliferating stem/progenitor cells (trypsinized from passaging dish, centrifuged, and resuspended). After one day of attachment to substrate, the proliferating stem/progenitor cells were then synchronously subjected to mitogen taper (= day 1); three 75% medium exchanges were carried out every other day with coculture differentiation solution containing 2% fetal bovine serum, 0.5 μM all-trans retinoic acid (prepared freshly on day of use), 10 μM forskolin, and 20 ng/ml NT3. Mitotic inhibitor FUDR (5-fluoro-2′-deoxyuridine) was included with uridine at 0.3 mM unless otherwise indicated at the start of the sixth day post-plating, after cell cycle exit and initiation of differentiation, to allow for long term culture (in some experiments 50 μM D-AP5 (RBI) was also included as noted in the text). Thereafter cultures were supplemented with NT3 (to 20 ng/mL) every 2-3 days until cocultures were 9-16 days old, at which point neurogenesis assays were performed.

Excitation of stem/progenitor cells in coculture

Stimuli were started on day 1 along with the initiation of mitogen taper and were included in the three 75% solution exchanges: added 50 μM glutamate, added 16 mM KCl, or added 16 mM NaCl as an osmotic control. Divalent cation concentration was maintained constant in external calcium variation experiments by replacement with equimolar magnesium. Nifedipine (RBI) was used at 10 μM and FPL 64176 at 5 μM. Persistent stimuli were used except where noted, to mimic areas of local persistent high activity and to avoid rebound or washoff effects. For brief stimuli, sham medium changes were conducted for control purposes with no neurogenic effect, and medium was fully replaced for the stimulation and removal of stimulation. An advantage of using depolarization for these brief stimuli is that the logarithmic dependence of depolarization on extracellular potassium described by the Nernst equation obviates the need for extensive washing of the stimulated sample prior to reapplication of the control medium.

Electrophysiology

Electrophysiology was carried out essentially as described (Deisseroth et al., 1996). Whole-cell recordings were obtained with an Axopatch 1D amplifier (Axon Instruments), NIDAQ National Instruments A/D board, and Igor Pro acquisition software. Cells were visualized on an inverted Nikon microscope with mercury arc lamp attachment. Morphologically, the most neuronal GFP+ cells (phase-bright somata with 2-5 primary processes) present in each condition were selected for recording. For miniature EPSC acquisition, cells were held at –70 mV in voltage clamp; for evoking sodium currents cells were held at –70 mV and stepped to –10 mV. The chamber was perfused with Tyrode's solution containing 129 mM NaCl, 5 mM KCl, 2 mM $CaCl_2$, 1 mM

$MgCl_2$, 30 mM glucose, 25 mM HEPES, and 10 μM glycine (pH 7.3 and osmolarity 313 ± 2 mOsm). Whole-cell patch electrodes (3–8 MΩ resistance) were filled with a solution containing 110 mM $CsMeSO_4$, 5 mM $MgCl_2$, 10 mM NaCl, 0.6 mM EGTA, 2 mM ATP, 0.2 mM GTP, and 40 mM HEPES (pH 7.2, 295 ± 2 mOsm), unless otherwise noted. TTX (from Calbiochem) at 1 μM was applied and washed via custom designed perfusion pipes positioned by the patched cell.

Immunocytochemistry

Cells were fixed in 4% formaldehyde (EM Sciences)/PBS for 20-30 min, washed 3x5 min in PBS/0.1M glycine, permeabilized for 5 min in 0.1% Triton/PBS/3% BSA, washed 3x5 min in PBS/glycine, blocked for 1-2 hr in PBS/3% BSA, and incubated overnight at 4ºC in PBS/3%BSA/ primary antibodies. Cells were then washed 3x5 min in PBS, incubated for 1 hr at 37ºC in PBS/3%BSA/secondary antibodies, washed 3x10 min in PBS, and mounted in Fluoromount (Electron Microscopy Sciences). TUNEL staining was performed with Apoptag Red (Serologicals). MAP2ab monoclonal Ab clone AP20 (Sigma) was used at 1:500, Doublecortin Ab (Santa Cruz Biotechnology) at 1:750, BrdU Ab (Accurate) at 1:500, and secondary Abs from Jackson Immunoresearch at 1:1000.

Confocal imaging and analysis

Images were acquired on a Zeiss LSM confocal microscope. Random fields containing GFP+ cells were selected for acquisition under GFP excitation without knowledge of experimental condition, and subsequently scanned using laser lines appropriate to excite the fluorophores corresponding to MAP2ab and other antigens. Data were analyzed using Metamorph software from Universal Imaging. MAP2ab or Dcx fluorescence values were obtained for each GFP+ cell

by quantifying the mean intensity of the corresponding fluorophore pixels overlying GFP+ pixels; occasional cells were excluded during analysis if they were found to be overlaid with MAP2ab positive processes from other nearby cells. Histograms of resulting values were generated for each experiment and MAP2ab-positivity threshold values for the fractional neurogenesis criterion were identified from the histograms, which show in the unstimulated case (as in Figure 1I) a sufficiently bimodal character allowing a threshold expression level to be set. Mean data from 12 independent experiments conducted with potassium depolarization were used as the reference point for effects of pharmacological interventions in coculture. For evaluation of proliferation and survival effects, daily cell counts as well as TUNEL and BrdU staining were performed in parallel stimulated and unstimulated cultures. BrdU was applied to cultures at 5 μM for 2 hr, and BrdU staining was conducted with a 20-30 min postfixation and subsequent incubation at 37°C for 20-30 minin 1N HCl. For Ca^{2+} imaging, x-Rhod-1 AM (Molecular Probes) was loaded at 10 μM for 30 min at 37°C into cells on the fixed coculture substrate 1-2 days after initiation of mitogen taper. Solutions for resting and stimulated cases corresponded to the differentiation solutions described above, and values shown represent mean somatic x-Rhod-1 fluorescence averaged over all observed cells. 100% of the cells imaged are represented in the averages. 44/73 cells showed an increase with glutamate, and 39/50 with depolarization. The actual number of responders is likely higher, as it is known that small juxtamembranous calcium elevations on the sub-micron scale (not detectable by imaging) couple robustly to intracellular signaling processes, particularly in the case of NMDA receptor and $Ca_v1.2/1.3$-mediated events (Deisseroth, 1998). Indeed, D-AP5 and nifedipine reduced Ser-133 phospho-CREB levels in the undifferentiated proliferating cells, providing another independent assay for both the presence of these channels on the proliferating stem/progenitors and their ability to couple effectively to

intracellular signaling pathways (not shown), in addition to blocking the rapid bHLH gene response to excitation (Figure 5) in the proliferating stem/progenitors.

Total RNA isolation, cDNA synthesis, and SYBR Green real-time quantitative RT-PCR

Total RNA was isolated using RNeasy mini kit (Qiagen) and synthesis of cDNA was performed using the SuperScript First-strand Synthesis System for RT-PCR (Invitrogen) following the manufacturers' instructions. Quantitative SYBR Green real time PCR was carried out as described previously (Mitrasinovic et al., 2001). Briefly, each 25µl SYBR green reaction consisted of 5 µl of cDNA (50ng/µl), 12.5 µl of 2x Universal SYBR Green PCR Master Mix (PerkinElmer Life Sciences) and 3.75 µl of 50 nM forward and reverse primers. Optimization was performed for each gene-specific primer prior to the experiment to confirm that 50nM primer concentrations did not produce nonspecific primer-dimer amplification signal in no-template control tubes. Primer sequences were designed using Primer Express Software. Quantitative RT-PCR was performed on ABI 5700 PCR instrument (PerkinElmer Life Sciences) by using 3-stage program parameters provided by the manufacturer as follows; 2 min at 50˚C, 10 min at 95˚C, and then 40 cycles of 15 s at 95˚C and 1 min at 60 ˚C. Specificity of the produced amplification product was confirmed by examination of dissociation reaction plots. A distinct single peak indicated that single DNA sequence was amplified during PCR. In addition, end reaction products were visualized on ethidium bromide-stained 1.4% agarose gels. Appearance of a single band of the correct molecular size confirmed specificity of the PCR. Each sample was tested in five copies with quantitative PCR, and samples obtained from three independent experiments were used to calculate the means and standard deviations. Primers were as follows (F=forward, R=reverse):

GAPDH F	AAGAGAGAGGCCCTCAGTTGCT
GAPDH R	TTGTGAGGGAGATGCTCAGTGT
MASH1 F	GACAGGCCCTACTGGGAATG
MASH1 R	CGTTGTCAAGAAACACTGAAGACA
HES1 F	CGGCTTCAGCGAGTGCAT
HES1 R	CGGTGTTAACGCCCTCACA
HES5 F	GGAGGCGGTGCAGTTCCT
HES5 R	GGAGTGGTAAAGCAGCTTCATC
ID2 F	ACAACATGAACGACTGCT
ID2 R	ATTTCCATCTTGGTCACC
NEUROD F	GGACAGACGAGTGCCTCAGTTC
NEUROD R	TCATGGCTTCAAGCTCATCCTCCT

Layered Hebbian neural network

Key characteristics of the model network are noted below; C source code is available on request. The aim of the model is to explore the effects which excitation-neurogenesis coupling could have on a memory-storage neural network (and not to precisely mimic a particular preparation, though key parallels to hippocampal functioning are included). The network consists of three layers with feedforward, full synaptic connectivity; the output layer activity pattern can be readily conceived of as a stable equilibrium of neuronal activity (according to some theories analogous to the brain state during active remembering), for example with neurons therein capable of persistent activity or participating in simple recurrent connections.

In the results presented there were 500 neurons per layer and neurogenesis with cell turnover permitted only at the middle "dentate gyrus" layer. For modeling clearance of old memories in Fig. 6G, turnover fraction was 0.05 for every 50 new patterns stored; for cell death, neurons were selected randomly. As newborn neurons must make functional connections in order to learn, such new neurons were allowed full connectivity to the presynaptic and postynaptic layers after being born, and allowed to learn subsequent patterns like the other neurons.

Synaptic connections were excitatory and neurons were simple threshold elements with binary activation values $\xi = 0$ or 1. As in the hippocampus, pattern representations were sparse; here, fraction of active neurons per pattern or sparsity (α) = 0.02 in all layers. Synaptic weights J between neurons i and j were set with the standard Hebb rule (Willshaw, 1969; Graham et al., 1999), $J_{ij} = \Sigma(\xi_i * \xi_j)$, summed over all stored patterns. Activity was propagated through the network in the usual manner, with only the first layer of each stored pattern provided (via the input layer) and activity of the second and third layer determined iteratively as the network attempts to reconstruct the full memory. A given cell j was determined to be active in a reconstructed memory if the incoming activity $\Sigma(\xi_i * J_{ij})$ summed over all presynaptic neurons i into that cell exceeded a threshold $\theta_j = \alpha_i * n_i$, where n_i is the total number of neurons in the j-1 layer and α_i is the sparsity of the j-1 layer. Efficacy of memory recall was judged by similarity of the output (third layer) activity pattern compared with the actual stored pattern; each incorrectly active or incorrectly inactive neuron increments the Hamming distance error metric by one unit.

Supporting references and notes

K. Deisseroth, H. Bito, R. W. Tsien, *Neuron* **16**, 89-101. (1996).
K. Deisseroth, E. K. Heist, R. W. Tsien, *Nature* **392**, 198-202. (1998).

B. Graham, D. Willshaw, *Neural Comput* **11**, 117-37. (1999).
H. A. Jinnah *et al.*, *Mov Disord* **15**, 542-51. (2000).
M. L. Monje, S. Mizumatsu, J. R. Fike, T. D. Palmer, *Nat Med* **8**, 955-62. (2002).
O. M. Mitrasinovic *et al.*, *J Biol Chem* **276**, 30142-9. (2001).
A. Okada, R. Lansford, J. M. Weimann, S. E. Fraser, S. K. McConnell, *Exp Neurol* **156**, 394-406. (1999).
T. D. Palmer, J. Takahashi, F. H. Gage, *Mol Cell Neurosci* **8**, 389-404 (1997).
T. D. Palmer, E. A. Markakis, A. R. Willhoite, F. Safar, F. H. Gage, *J Neurosci* **19**, 8487-97. (1999).
D. J. Willshaw, O. P. Buneman, H. C. Longuet-Higgins, *Nature* **222**, 960-2. (1969).

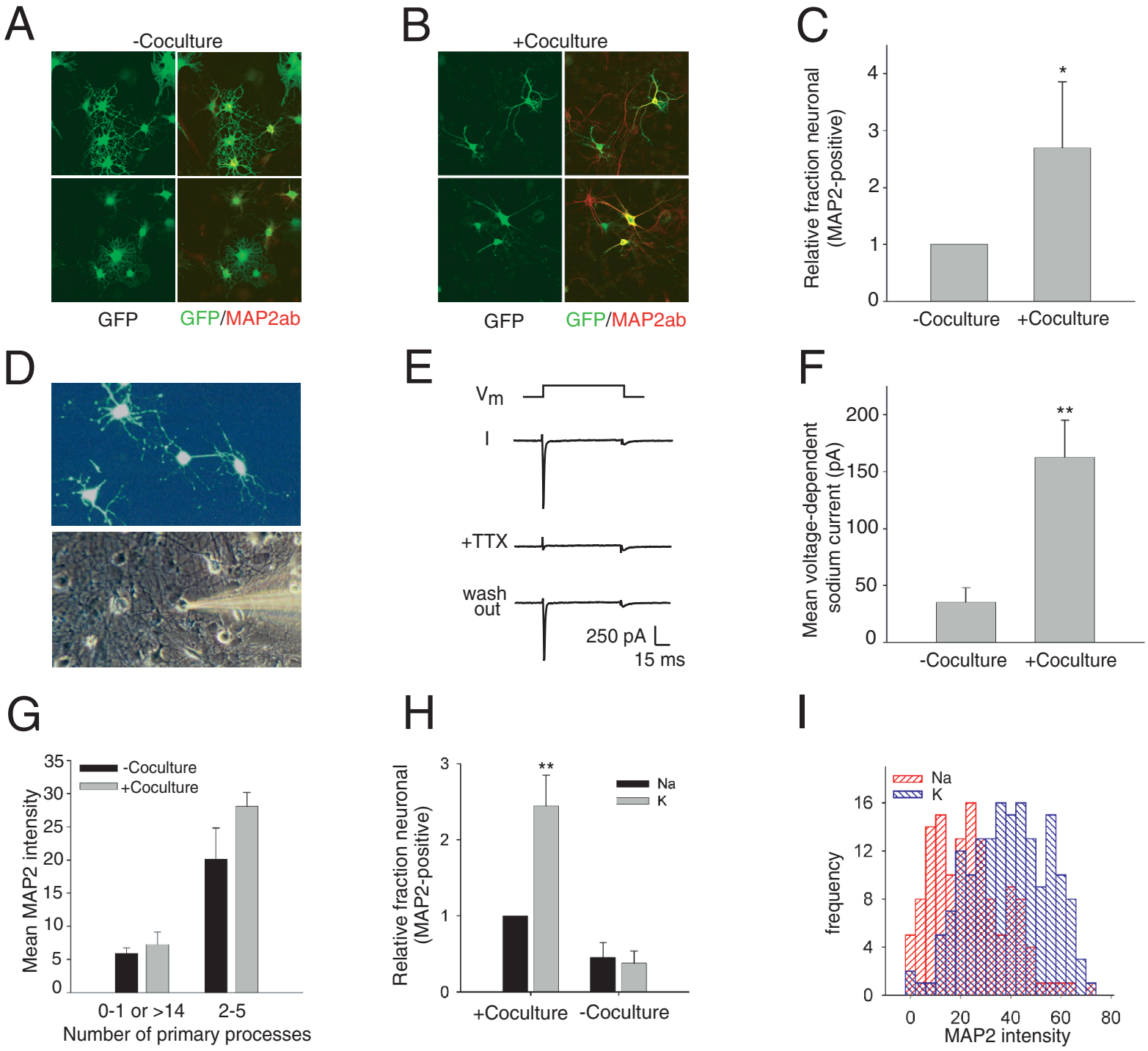
A
-Coculture
GFP
GFP/MAP2ab
B
+Coculture
GFP
GFP/MAP2ab
C
Relative fraction neuronal (MAP2-positive)
0
1
2
3
4
*
-Coculture
+Coculture
D
E
Vm
I
+TTX
wash out
250 pA
15 ms
F
Mean voltage-dependent sodium current (pA)
0
50
100
150
200
**
-Coculture
+Coculture
G
Mean MAP2 intensity
0
5
10
15
20
25
30
35
-Coculture
+Coculture
0-1 or >14
2-5
Number of primary processes
H
Relative fraction neuronal (MAP2-positive)
0
1
2
3
**
Na
K
+Coculture
-Coculture
I
frequency
0
4
8
12
16
Na
K
0
20
40
60
80
MAP2 intensity

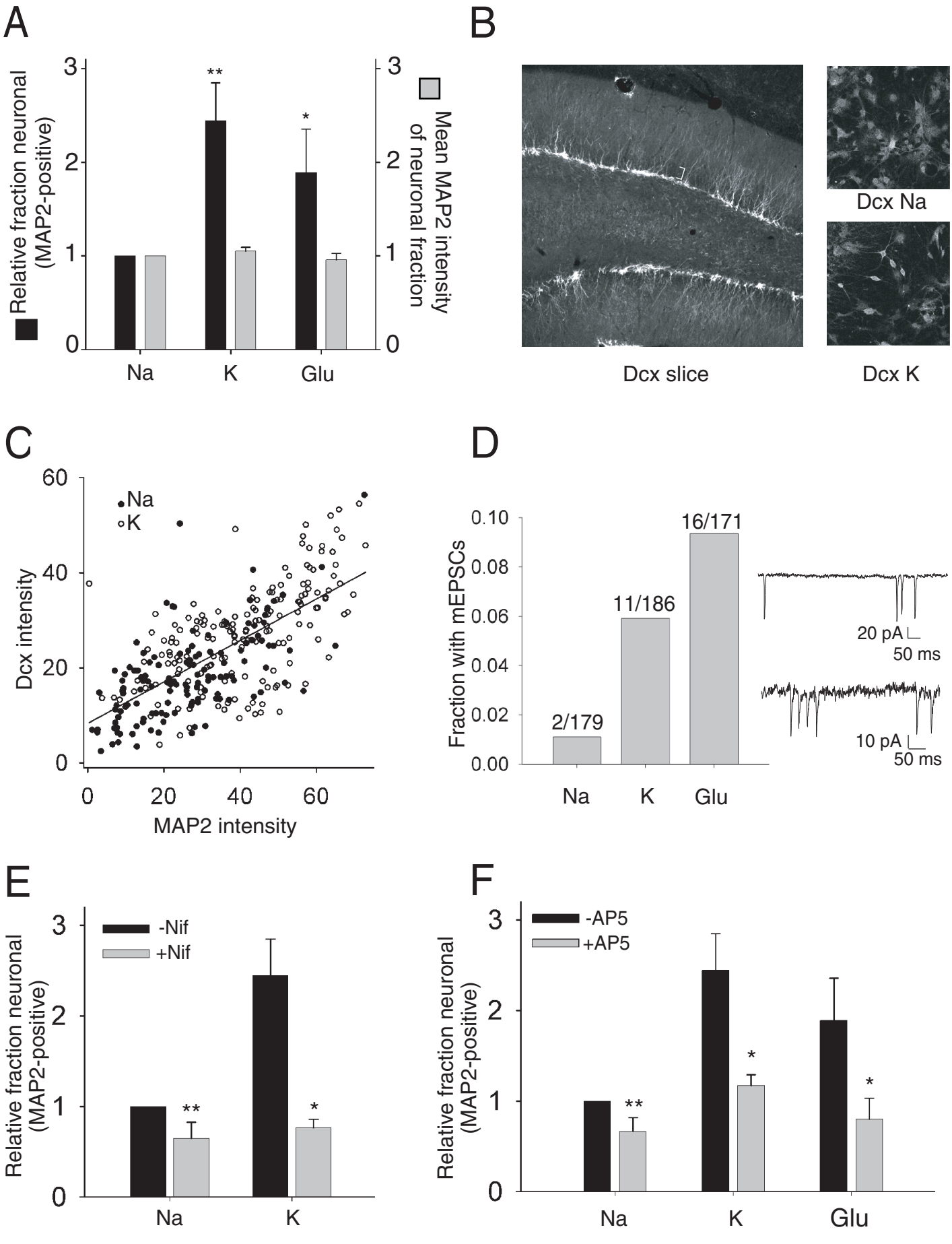
A
Relative fraction neuronal (MAP2-positive)
Mean MAP2 intensity of neuronal fraction
**
*
Na
K
Glu
B
Dcx slice
Dcx Na
Dcx K
C
Na
K
Dcx intensity
MAP2 intensity
D
Fraction with mEPSCs
2/179
11/186
16/171
20 pA
50 ms
10 pA
50 ms
Na
K
Glu
E
-Nif
+Nif
Relative fraction neuronal (MAP2-positive)
Na
K
F
-AP5
+AP5
Relative fraction neuronal (MAP2-positive)
Na
K
Glu

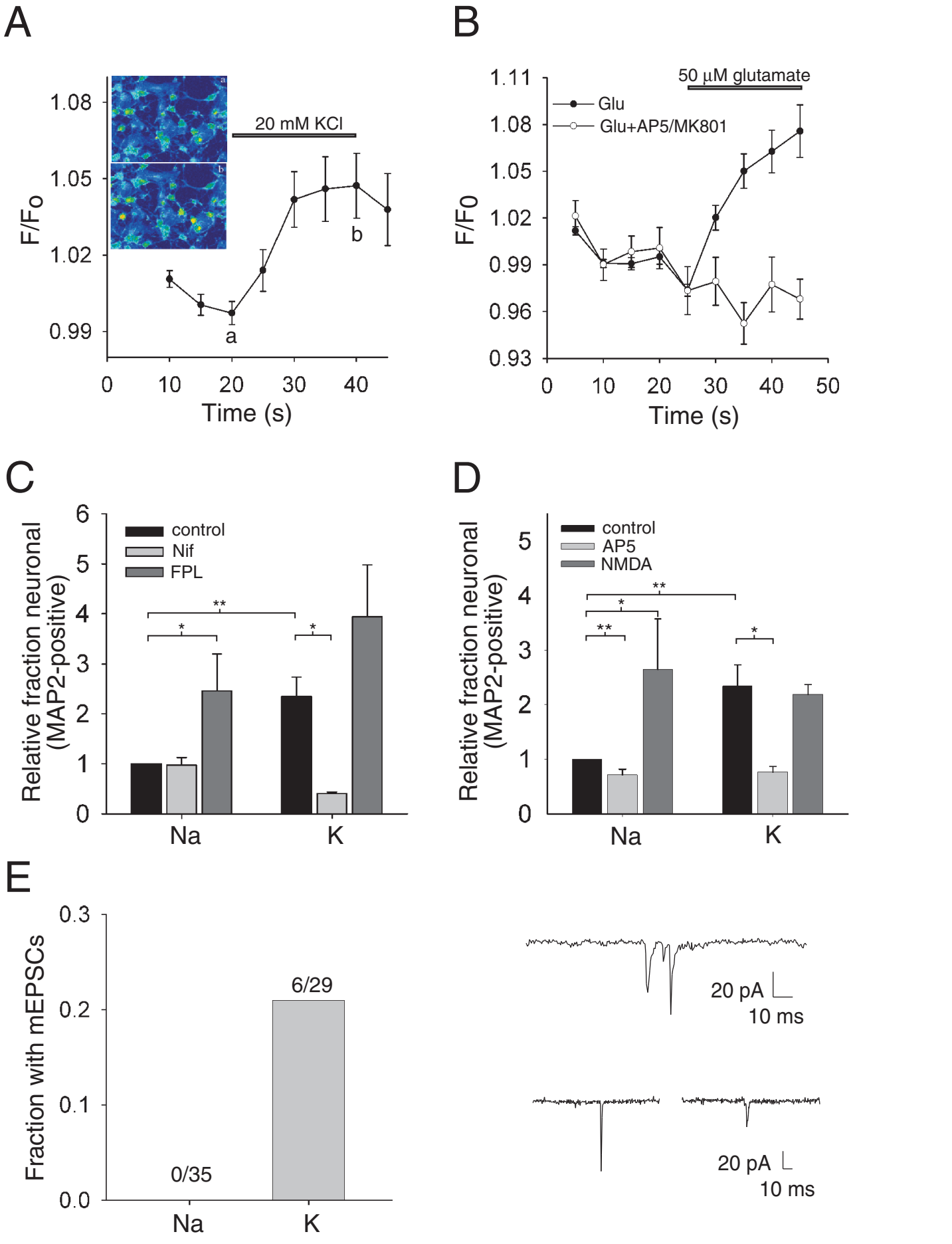
A
1.08
1.05
1.02
0.99
F/Fo
20 mM KCl
a
b
0
10
20
30
40
Time (s)
B
1.11
1.08
1.05
1.02
0.99
0.96
0.93
F/F0
50 µM glutamate
Glu
Glu+AP5/MK801
0
10
20
30
40
50
Time (s)
C
Relative fraction neuronal (MAP2-positive)
control
Nif
FPL
Na
K
D
Relative fraction neuronal (MAP2-positive)
control
AP5
NMDA
Na
K
E
Fraction with mEPSCs
0.3
0.2
0.1
0.0
0/35
6/29
Na
K
20 pA
10 ms
20 pA
10 ms

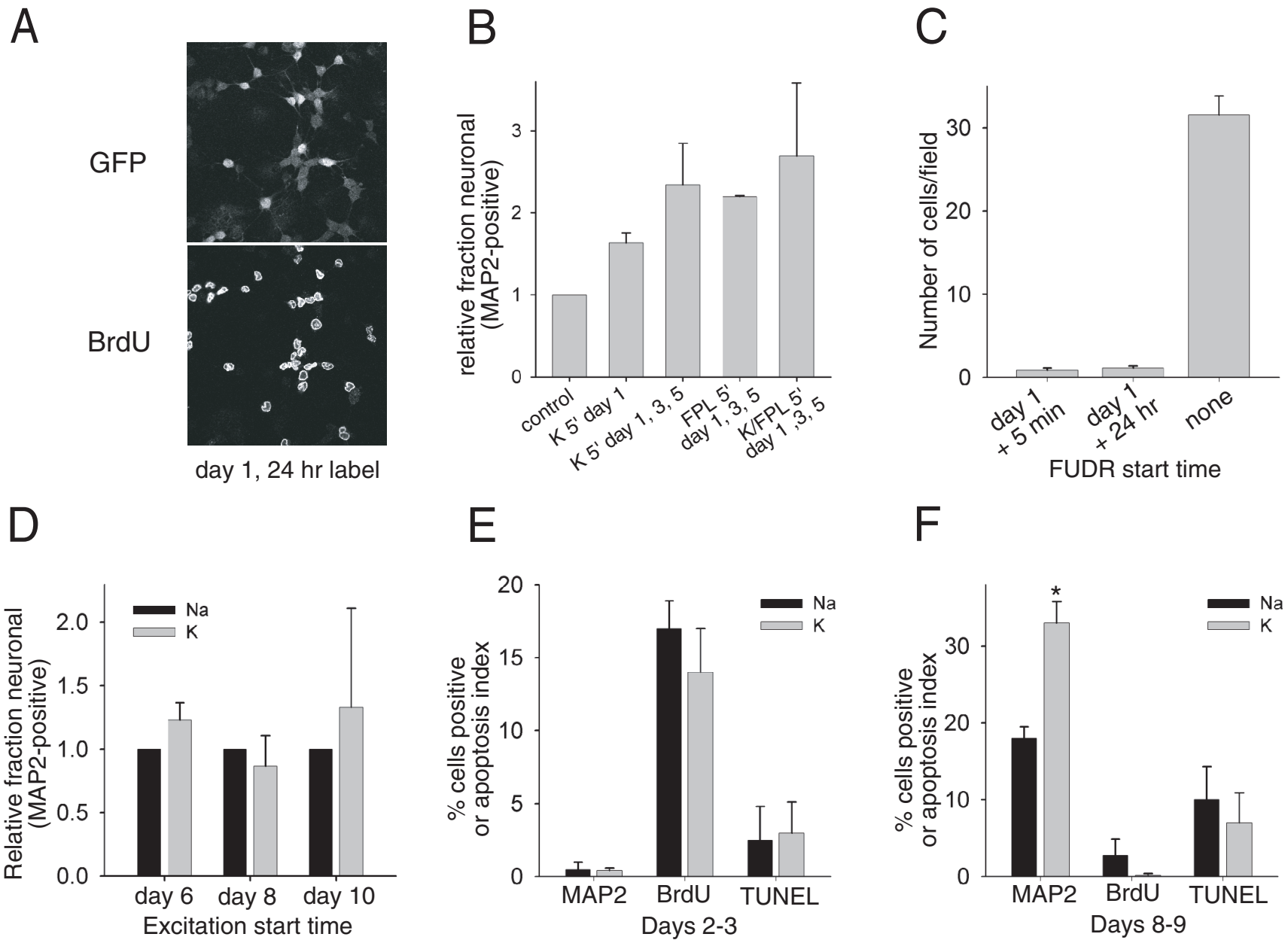
A
GFP
BrdU
day 1, 24 hr label
B
relative fraction neuronal (MAP2-positive)
0
1
2
3
control
K 5' day 1
K 5' day 1, 3, 5
FPL 5' day 1, 3, 5
K/FPL 5' day 1 ,3, 5
C
Number of cells/field
0
10
20
30
day 1 + 5 min
day 1 + 24 hr
none
FUDR start time
D
Relative fraction neuronal (MAP2-positive)
0.0
0.5
1.0
1.5
2.0
Na
K
day 6
day 8
day 10
Excitation start time
E
% cells positive or apoptosis index
0
5
10
15
20
Na
K
MAP2
BrdU
TUNEL
Days 2-3
F
% cells positive or apoptosis index
0
10
20
30
*
Na
K
MAP2
BrdU
TUNEL
Days 8-9

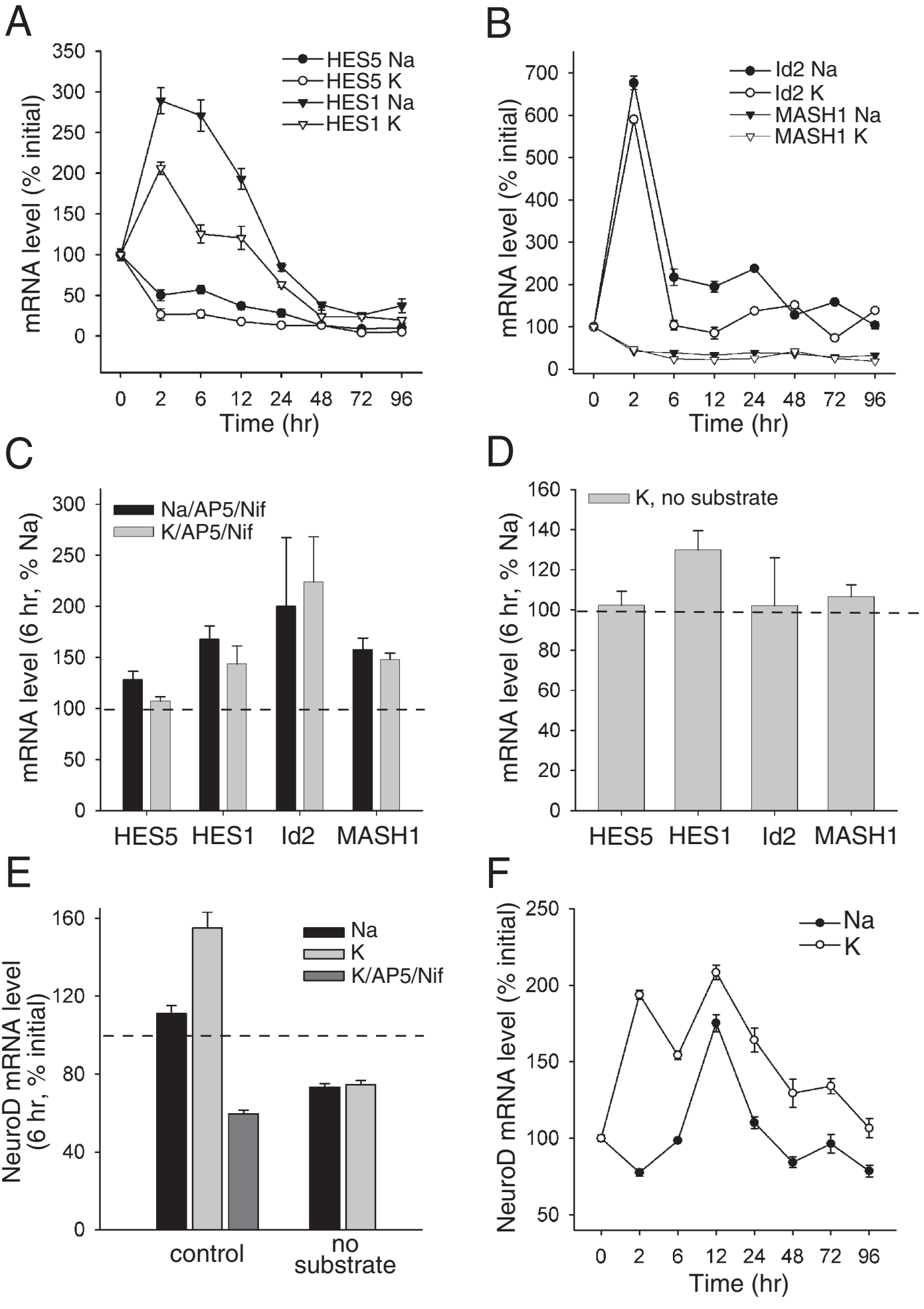
A
mRNA level (% initial)
HES5 Na
HES5 K
HES1 Na
HES1 K
Time (hr)
B
mRNA level (% initial)
Id2 Na
Id2 K
MASH1 Na
MASH1 K
Time (hr)
C
mRNA level (6 hr, % Na)
Na/AP5/Nif
K/AP5/Nif
HES5
HES1
Id2
MASH1
D
mRNA level (6 hr, % Na)
K, no substrate
HES5
HES1
Id2
MASH1
E
NeuroD mRNA level (6 hr, % initial)
Na
K
K/AP5/Nif
control
no substrate
F
NeuroD mRNA level (% initial)
Na
K
Time (hr)

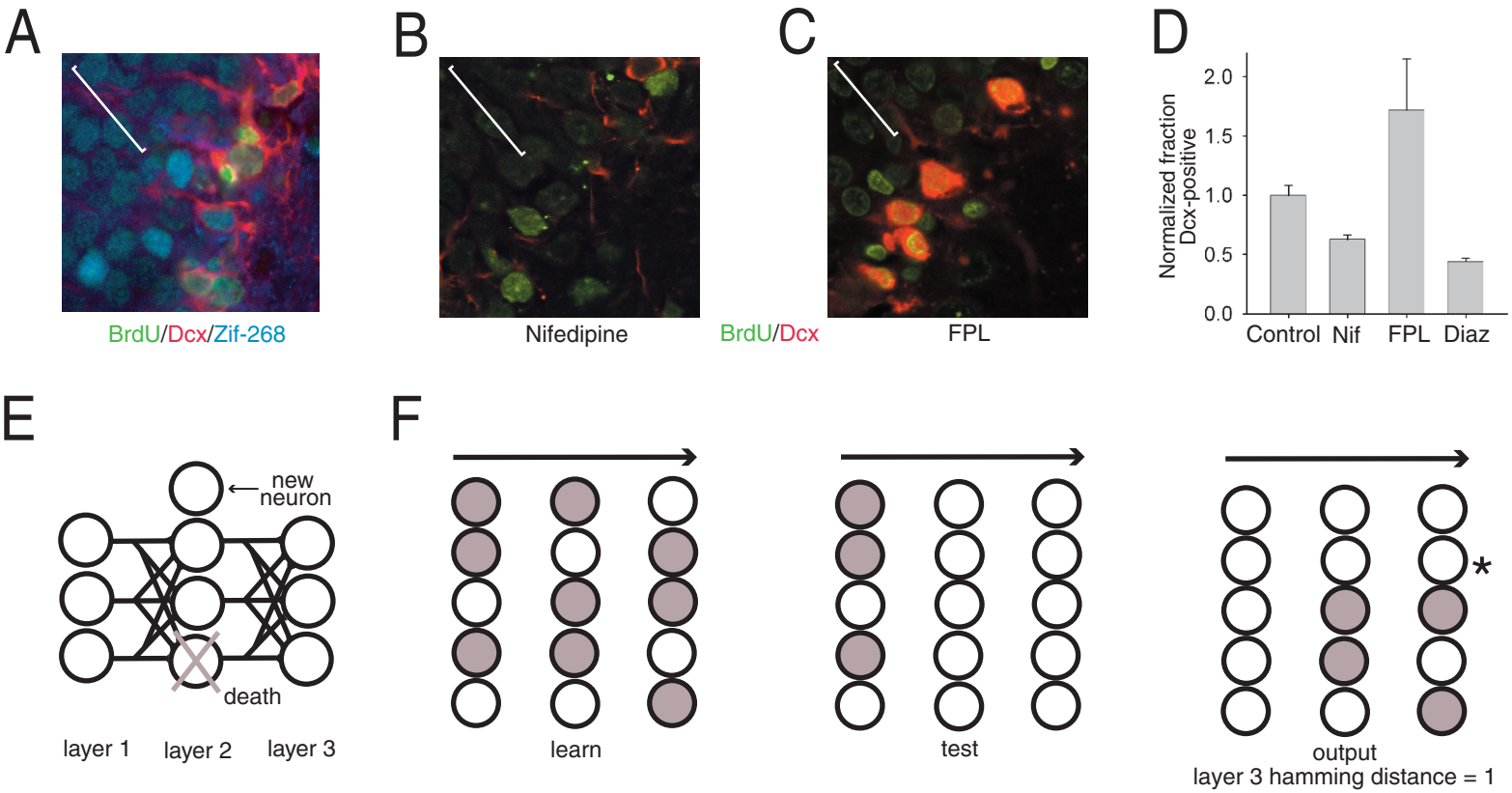
A
BrdU/Dcx/Zif-268
B
Nifedipine
C
BrdU/Dcx
FPL
D
Normalized fraction Dcx-positive
2.0
1.5
1.0
0.5
0.0
Control
Nif
FPL
Diaz
E
new neuron
death
layer 1
layer 2
layer 3
F
learn
test
output
layer 3 hamming distance = 1
*
G
old memories
stable
neurogenesis
Hamming distance (layer 3)
Time post-learning
H
new memories
stable
neurogenesis
Hamming distance (layer 3)
Network activity level
I
Relative fraction neuronal (MAP2-positive)
0
0.3
0.6
0.9
1.2
1.5
1.8
[Ca2+]o, mM